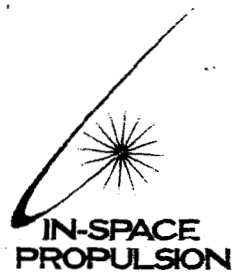

Modeling of Spacecraft

Advanced Chemical Propulsion Systems

Michael P.J. Benfield
Jeremy A. Belcher
Science Applications International Corporation,
Huntsville, Alabama, 35806

The work described in this paper was funded in whole or in part by the In-Space Propulsion Technology Program, which is managed by NASA's Science Mission Directorate in Washington, D.C., and implemented by the In-Space Propulsion Technology Office at Marshall Space Flight Center in Huntsville, Ala. The program objective is to develop in-space propulsion technologies that can enable or benefit near and mid-term NASA space science missions by significantly reducing cost, mass or travel times.

Modeling of Spacecraft Advanced Chemical Propulsion Systems

Michael P.J. Benfield* and Jeremy A. Belcher†
Science Applications International Corporation, Huntsville, Alabama, 35806

This paper outlines the development of the Advanced Chemical Propulsion System (ACPS) model for Earth and Space Storable propellants. This model was developed by the Systems Technology Operation of SAIC-Huntsville for the NASA MSFC In-Space Propulsion Project Office. Each subsystem of the model is described. Selected model results will also be shown to demonstrate the model's ability to evaluate technology changes in chemical propulsion systems.

Nomenclature

ACS	=	attitude control system
A_{TP}	=	surface area of propellant tank, m^2
C_{MLI}	=	constant from the literature, kg/m^2-layer
DOP	=	depletion of propellant
D_{TP}	=	propellant tank diameter, m
D_{TPF}	=	fuel tank diameter, m
D_{TPMAX}	=	larger of fuel or oxidizer tank diameter, m
D_{TPOX}	=	oxidizer tank diameter, m
F_{PMD}	=	propellant management device volume factor, > 1.0
F_{REG}	=	ratio of regulator inlet to outlet pressure at DOP, >1.0 (baseline value of 1.5)
F_U	=	ullage factor, >1.0
g_O	=	universal gravitational constant, 9.80665, m/sec^2
Isp	=	propellant combination specific impulse, sec
M_{ACS}	=	total mass of monopropellant ACS, kg
M_{BT}	=	total blanket mass of system, kg
M_{CAB}	=	cable harness mass, kg
M_{CE}	=	mass of cryocooler control electronics, kg
M_{CRR}	=	mass of cryocooler radiator, kg
M_{CRY}	=	mass of cryocooler, kg
M_{DIST}	=	distribution element (in propellant/pressurant feed system) mass, kg
M_F	=	fuel mass, kg
M_{GC}	=	ground cooling mass penalty for cryogenic propellant, kg
M_{HDOP}	=	mass of gaseous helium in propellant and pressure tanks at DOP, kg
M_{HPDOP}	=	mass of gaseous helium in propellant tank at DOP
MLI	=	multi-layer insulation
M_O	=	launch mass, kg
M_P	=	total propellant mass, kg
M_{PACS}	=	mass of monopropellant for ACS, kg
M_{POW}	=	mass of power system required for cryocooling, kg
MR	=	mixture ratio, mass of oxidizer/mass of fuel
M_{SP}	=	primary structure mass, kg
M_{SS}	=	propulsion subsystem structure mass, kg
M_{TCRS}	=	mass of soft cryogenic propellant cryocooling subsystem, kg
M_{TPC}	=	mass of composite propellant tank, kg

* Systems Engineer, Systems Technology Operation, 675 Discovery Drive, Huntsville, AL 35806, AIAA Member.
† Junior Engineer, Systems Technology Operation, 675 Discovery Drive, Huntsville, AL 35806, AIAA Member.

M_{TLAE} = mass of main engines and associated mounts and heat shields, kg
M_{TPT} = mass of titanium propellant tank, kg
N_{LAE} = number of main engines
N_{LEGS} = number of distribution lines in propellant/pressurant feed system
N_{MLIP} = number of layers of MLI assumed for propellant tank
N_{MLIT} = number of layers of MLI assumed to cover entire propulsion system
P_{TP} = propellant tank pressure, psia
R_{HE} = helium gas constant, 2077.25 J/kg-K
S_{ACP} = stress margin in propellant tank composite (assumed 1.0 in AXAF-I)
T = main engine thrust level, N
T_C = cold head temperature, K
T_E = environmental temperature for specific mission/system, K
T_{LP} = tank liner thickness, m
T_{THDOP} = temperature of helium tank at DOP, K
ΔV = velocity required for maneuver, m/sec
V_{TPHDOP} = volume of expelled propellant, m^3
W_C = cooling power, W
W_{IN} = power into cryocooler, W
Wt = rejected heat, W
Z = compressibility factor representing departures from ideal gas performance
α_{POW} = specific mass of the power system, kg/W
ρ_{AFP} = areal density of propellant tank foam, kg/m^2
ρ_{AP} = propellant management device areal density, kg/m^2
ρ_F = fuel density, kg/m^3
ρ_{HBOM} = helium density, kg/m^3
ρ_{LP} = density of propellant tank liner, kg/m^3
ρ_{OX} = oxidizer density, kg/m^3
ρ_P = propellant density, kg/m^3

I. Introduction

The ACPS was developed by the Systems Technology Operation of SAIC-Huntsville for the NASA MSFC In-Space Propulsion Project Office. It was created to give a means to evaluate advanced Earth and space storable chemical propulsion systems for missions of interest. The model is intended to provide for rapid and accurate estimates of the key characteristics and performances of advanced chemical propulsion systems as functions of propulsion technology options and specific mission requirements. Overall ACPS architectures were based on recent studies and the successful AXAF-I and Cassini propulsion subsystems. Components were parametrically modeled using a combination of experience-based and State-of-the-Art (SOA) physics-based models. At the present, the model can evaluate a broad range of technology-options and mission combinations. A model modification planned that will add a hard cryogen propellant (LH_2) capability.

Figure 1 shows a diagram of the overall ACPS model. Initial inputs to the model include the mission profile (masses, delta-v's and spacecraft thermal environment) and selected subsystem options (propellant residuals, feed system pressure changes, etc.). There are 10 subsystems in the model as shown in Figure 1. The ACPS output represents a spacecraft for a given mission.

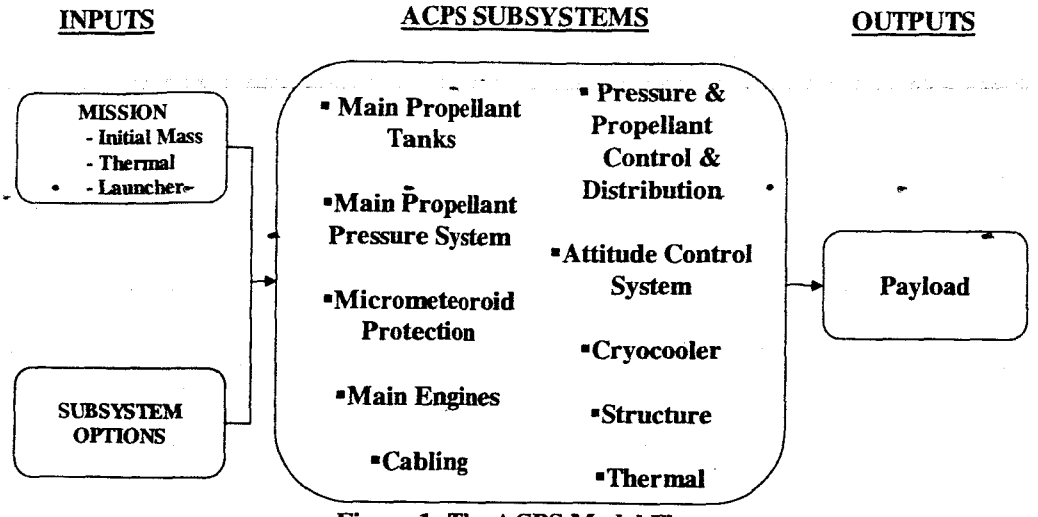

Figure 1: The ACPS Model Flow

II. Architectures

The ACPS architecture is based on the AXAF (Chandra) (Reference 1 and 2) and Cassini (Reference 3 and 4) propulsion systems, a recent study of planetary stages that included both soft cryogenic and Earth-storable propellant combinations (Reference 5), and a review of planetary spacecraft by the Lockheed Martin Corporation (Reference 6). Both Earth-storable and soft cryogen propellant systems were assumed to be relevant to the model. Options include a monopropellant as well as bi-propellant main engine system. Spherical tanks that were longitudinally located to one another were assumed for this model for comparison purposes. Pressurant tanks were also assumed to be nested with the propellant tanks.

III. Propellant Load

The propellant load for the mission is calculated by the Eq. (1).

$$M_P = M_O\left(1 - e^{\frac{-\Delta V}{g_O Isp}}\right) \tag{1}$$

Depending on the mission, several ΔV burns and mass additions (sample return) or mass deletions (lander separation) can be added in the appropriate sequence to determine the amount of propellant needed for a given mission profile. Once the amount of propellant has been determined for the mission, residuals and margins are then added. Knowing the mixture ratio of the propellants, the amount of oxidizer and fuel can then be determined for the main propellant tanks.

IV. Main Propellant Tanks

Once the propellant load of the oxidizer and fuel is known, the volume and mass of the main propellant tanks can be calculated. Figure 2 depicts the overall method for calculating the main propellant tank mass.

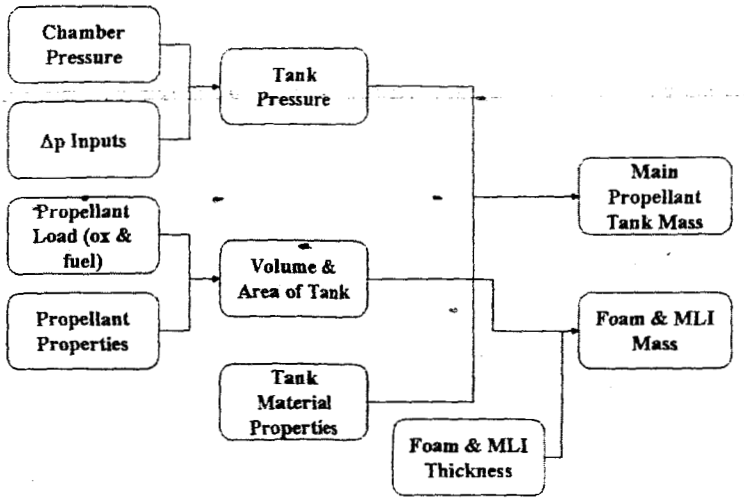

Figure 2: Main Propellant Tank Subsystem Flow.

The propellant tank pressure is a driver on tank mass and is derived from the main engine chamber pressure assumed. The feed system from the tank to the engine is assumed to have pressure drops associated with the engine injector, a venturi value, and lines. Those pressure drops are inputs to the system and can be changed to accommodate specific design approaches. Either a composite overwrap or titanium tank may be selected for evaluation.

For composite propellant tanks, the model is scaled from the AXAF-I propellant tanks with the mass of each composite tank calculated by Eq. (2).

$$M_{TPC} = 4.84\left\{8.9\ \ 10^{-7}\left[\left(F_{PMD}F_U\right)\left(\frac{M_P}{\rho_P}\right)\right]^{1/3}\left(P_{TP}S_{ACP}\right)+1.12\ \ 10^{-3}\left(T_{LP}\rho_{LP}\right)+0.89+C_{MLI}N_{MLIP}+\rho_{AFP}\right\}\left[\left(F_{PMD}F_U\right)\left(\frac{M_P}{\rho_P}\right)\right]^{2/3} \quad (2)$$

For Titanium tanks, the model is scaled from values for commercially available tanks obtained from Reference 7. Tank masses for various burst and operating pressures were selected. These masses included the propellant management devices (PMD). The tank masses were all linearly normalized to an operating pressure of 300 psia for this model. Having this data, a linear regression equation was created for tank mass as a function of tank diameter. Figure 3 shows the relationship between the titanium tank mass and the tank diameter.

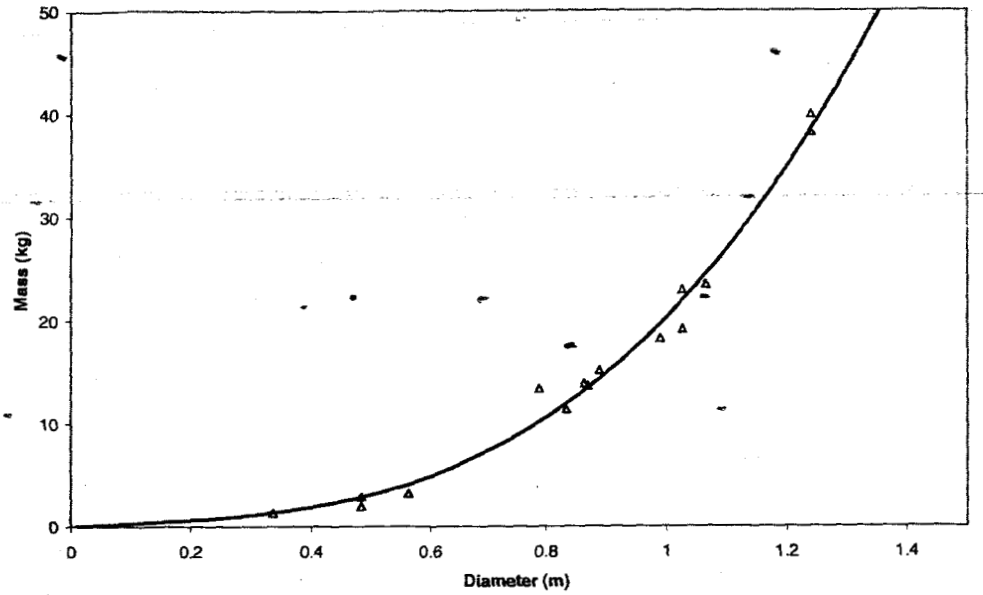

Figure 3: Titanium Shell Mass as a Function of Tank Diameter

From this figure, Eq. 3 can calculate taking the linear regression curve generated and knowing that the tanks were normalized to an operating pressure of 300 psia, the titanium tank mass.

$$M_{TPT} = \left(\frac{P_{TP}}{300}\right)\left[22.34(D_{TP})^3 - 5.50(D_{TP})^2 + 3.28(D_{TP})\right] \tag{3}$$

V. Propellant Pressurization

The method used for determining the amount of helium required to pressurize the system is taken from Reference 8. With the long burn of most of the systems of interest, the helium tank is assumed to undergo an isothermal expansion. Also, because nested tanks are envisioned for these spacecraft, it is assumed that the helium temperature will always equal the propellant temperature. Using this assumption and the information from Reference 8, Eq. (4) was developed to calculate the required helium amount.

$$M_{HDOP} = M_{HPDOP}\left(1 + \frac{F_{REG}P_{TP}}{ZR_{HE}T_{THDOP}\rho_{HBOM} - F_{REG}P_{TP}}\right) \tag{4}$$

$$M_{HPDOP} = \frac{P_{TP}V_{TPHDOP}}{ZR_{HE}T_{THDOP}} \tag{5}$$

VI. Main Engines

The main engine model was scaled from data from Reference 9. This was slightly modified to account for the heavier rhenium engines (Reference 10 and Reference 11) assumed herein. Rhenium engines were selected, as they are the highest performing engines available at the thrust levels of interest. Figure 4 shows the data obtained.

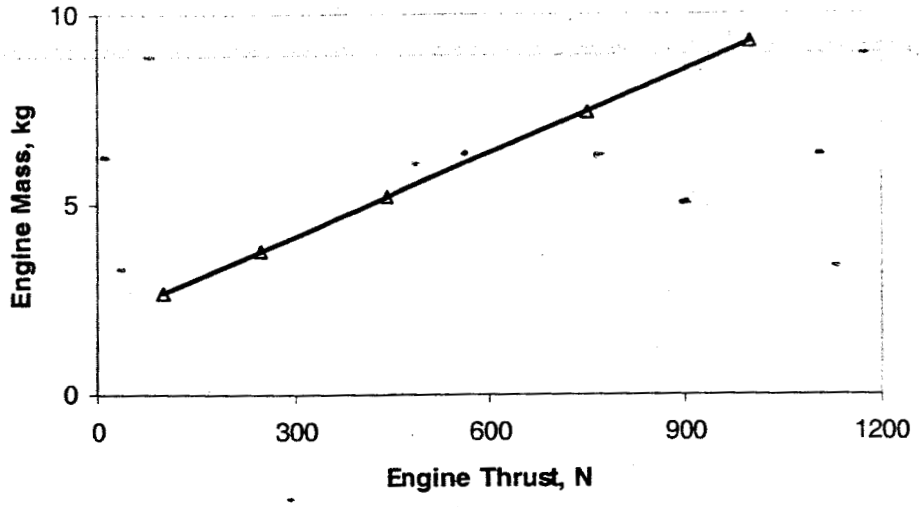

Figure 4: Engine Mass as a Function of Engine Thrust

Accounting for the engine mounts and heat shields results in Eq. (6), which calculates the mass of the main engines and the associated mounts and heat shields.

$$M_{TLAE} \approx N_{LAE} [0.013\ T + 3.43] \tag{6}$$

VII. Pressure and Propellant Control/Distribution

The propellant and pressurant control and distribution components were separately considered. The control components consisted of valves, regulators, and other components that influence the values of pressure and flow rate. The control components were assumed to be like those used on Cassini as they were representative of a highly reliable spacecraft. Minor modifications were made because of the separation of the pressurant tanks for the oxidizer and fuel assumed herein. The types and number of Earth and space-storable pressurant and propellant control elements were from the Cassini spacecraft (Reference 3). The masses of the Earth and space-storable pressurant and propellant control elements were from Reference 12. Table 1 shows the data for the propellant and pressurant components. The distribution elements consisted of lines, tie downs, heaters, and MLI, etc. associated with the distribution of the pressurant and propellant systems and the AXAF propulsion system was used as a reference for those elements

Table 1. Masses of Pressurant and Propellant Control Components

Number of Engines	Monopropellant		Bipropellant	
	Earth-storable	Cryogenic	Earth-storable	Cryogenic
1	12.61	-	23.66	43.99
2	14.17	-	25.22	47.08

Equation (7) calculates the mass of the distribution elements of the chemical system.

$$M_{DIST} \approx 2.37(N_{LEGS})\left\{(M_F)^{1/3}\left[\frac{(MR)\rho_F + \rho_{OX}}{\rho_F \rho_{OX}}\right]^{1/3}\right\} \tag{7}$$

VIII. Attitude Control System (ACS)

The attitude control system (ACS) was based on Cassini and was assumed to use hydrazine monopropellant system that utilized 12 fully redundant thrusters for three-axis stabilization. The required hydrazine propellant mass is extremely mission dependent, but was set as the same fraction of initial spacecraft mass as used for Cassini:

$$M_{PACS} = 0.0237(M_O) \tag{8}$$

Masses of the spherical propellant tanks were set as a fraction of the ACS propellant mass derived from a straight-line plot of the values on AXAF-I and Cassini. The mass of the distribution elements was taken from AXAF-I data modified to account for the different number of thrusters on Cassini. Incorporating all of the scaling performed, the final mass of the ACS is found by Eq. (9).

$$M_{ACS} = 0.025\ M_O + 18.7 \tag{9}$$

IX. Zero Boiloff (ZBO)

The cryocooler model is designed for zero-boiloff (ZBO). Historical cryocooler data were obtained from reference 5 and 6 as a basis for scaling the mass of a cryocooler for soft cryogens (LOX, F2, Methane, etc.). The total mass of the ZBO subsystem can was assumed to be the sum of cryocooler, control electronics, radiator, required power and a small cooling loop for ground operations as shown in Eq. (10).

$$M_{TCRS} = [\ M_{CRY} + M_{CE} + M_{CRR} + M_{POW} + M_{GC}] \tag{10}$$

The mass of the cryocooler itself is given by Eq. (11) (Reference 13).

$$M_{CRY} = 157\ EXP(-0.0533T_C)\ (W_C)^{(0.009Tc + 0.1275)} \tag{11}$$

The controller electronics mass was obtained from the lowest values of power processor specific mass in Reference 14. The controller electronics mass if given by Eq. (12).

$$M_{CE} = 0.02\ W_{IN} \tag{12}$$

The radiator mass was scaled from data taken from Reference 15. The model assumed a beryllium radiator, a view factor of 1 and was maintained at a temperature 30 degrees above the environmental temperature of the spacecraft. The mass of the radiator associated with the cryocooler system is given by Eq. (13).

$$M_{CRR} = (W_C + W_{IN}) f(Wt) \left[\frac{378}{T_E + 30}\right]^4 \left(\frac{1.5}{1.0}\right)(0.78) \tag{13}$$

The mass of the power system is given in Eq. (14) and M_{GC} was assumed to be a constant small mass.

$$M_{POW} = \alpha_{POW}\ W_{IN} \tag{14}$$

X. Thermal

The MLI and foam for the propellant tanks and the thermal control for the propellant distribution systems were accounted for in the model of those subsystems. Reference 16 provides for 13 layers of MLI over the entire structure of the propulsion system. For modeling purposes the area that requires these layers will be assumed to be a cylinder with a diameter that is 1.1 times larger than the larger of the fuel or oxidizer tank and a length that is 1.1 times the addition of the fuel and oxidizer tanks. Because of the tandem cylindrical tank approach for this architecture, this was assumed to model the entire propulsion system. Equation 15 calculates the mass of the thermal blankets assumed to cover the entire chemical propulsion system.

$$M_{BT} = C_{MLI} N_{MLIT} \left\{[2\pi][1.1(D_{TPMAX})][1.1](D_{TPF} + D_{TPOX}) + [2\pi][1.1(D_{TPMAX})]^2\right\} \tag{15}$$

XI. Structure

The structural model for the ACPS has two components: primary (load bearing) structure and secondary structure (tank supports). Data was obtained from a spacecraft manufacturer of several spacecraft of their primary and secondary structures as a function of their initial system mass and their propellant load (Reference 5). Linear regression curves were applied to each set of data. Figure 5 shows the primary structure as a function of initial system mass. Figure 6 depicts the relationship between secondary structure and propellant load.

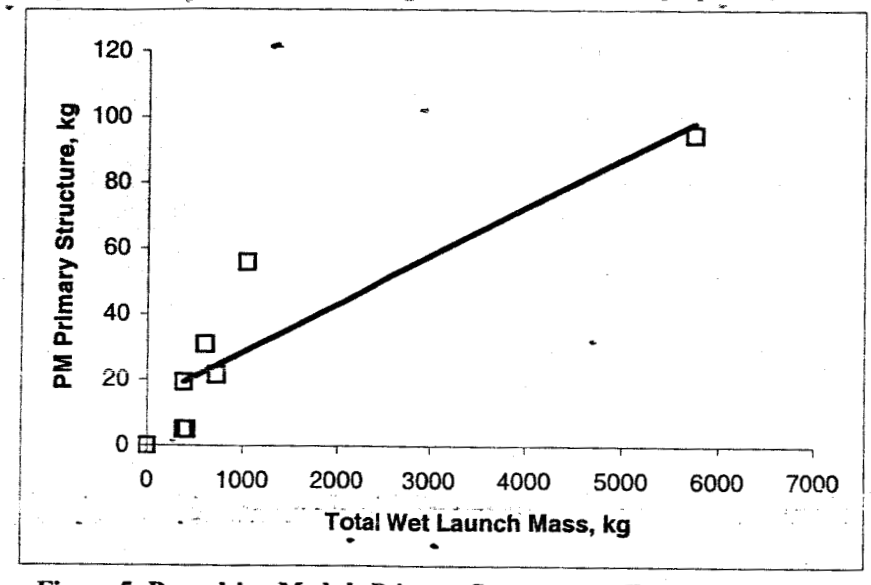

Figure 5: Propulsion Module Primary Structure vs. Total Launch Mass

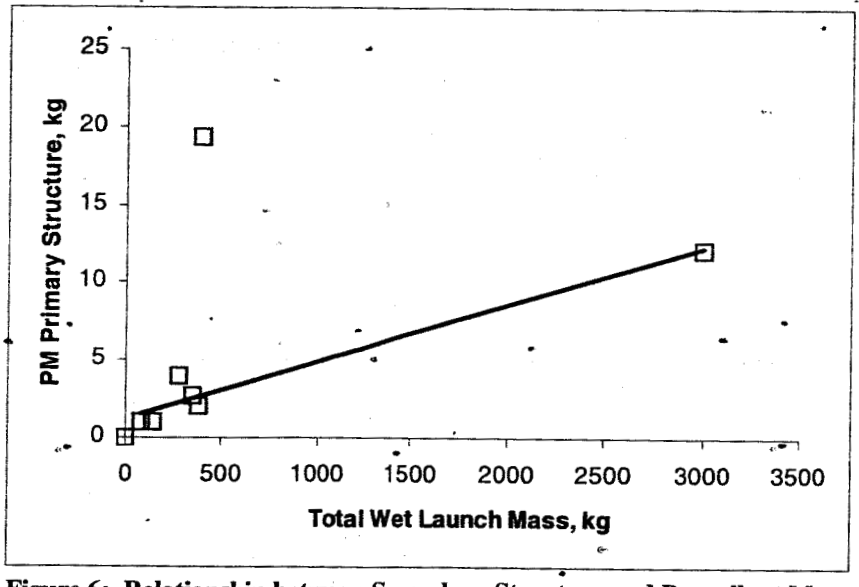

Figure 6: Relationship between Secondary Structure and Propellant Mass

From this curve fits, Eqs. (16) and (17) are derived to predict the mass of the structural subsystem for the ACPS.

$$M_{SP} = 0.0147(M_O) + 13.618 \quad (16)$$

$$M_{SS} = 0.0037(M_P) + 1.2401 \quad (17)$$

XII. Cabling

The cable harness for the ACPS is assumed to also vary with the linear dimension of the total propellant volume. Hence, the mass of the cable harness is given by Eq. (18).

$$M_{CAB} = 17.72(M_P)^{1/3}\left[\frac{(MR)\rho_F + \rho_{OX}}{\rho_F \rho_{OX}}\right]^{1/3} \qquad (18)$$

XIII. Selected Outputs

The ACPS has the capability to assess different propulsion technologies and mission requirements to determine their impact at the system level either in payload, system wet mass, or initial mass of the system. Small detailed effects such as the effect of the delta-pressure change from the cavitating venturi in the feed system can be shown at the system level. Figures are provided below that outline some of the capabilities of the model.

Figure 7 shows the detailed mass breakdown of the wet mass of several propellant combinations for a given Mo of 3000 kg and a ΔV of 2500 m/sec. By comparing several different propulsion combinations at once and giving the detailed mass breakouts, one can see where the advantages of a system are at the system level.

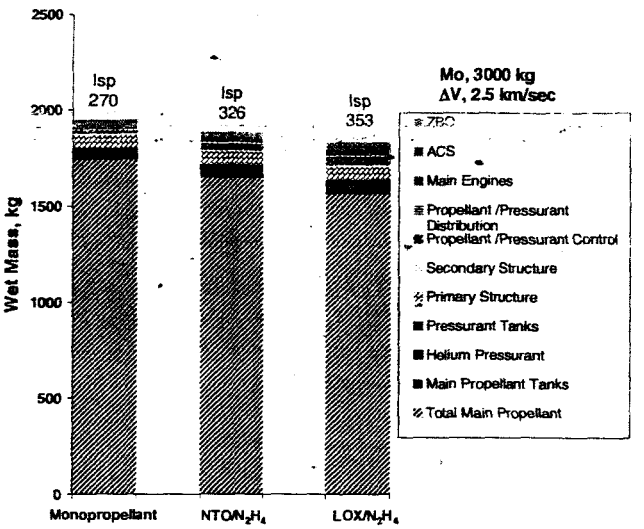

Figure 7: Wet Mass of Selected Propellant Combinations

Figure 8 depicts the effect of both raising the combustion chamber temperature of a NTO/N2H4 engine (either by raising the chamber pressure or the mixture ratio) and advancing the state-of-the-art in tank technologies. Given a mission requirement of a Mo of 2000 kg and a ΔV of 2000 m/sec, the results indicate in Figure 8 that either changing the mixture ratio or advancing tank technologies will increase payload. Increasing chamber pressure alone does not have the desired effect.

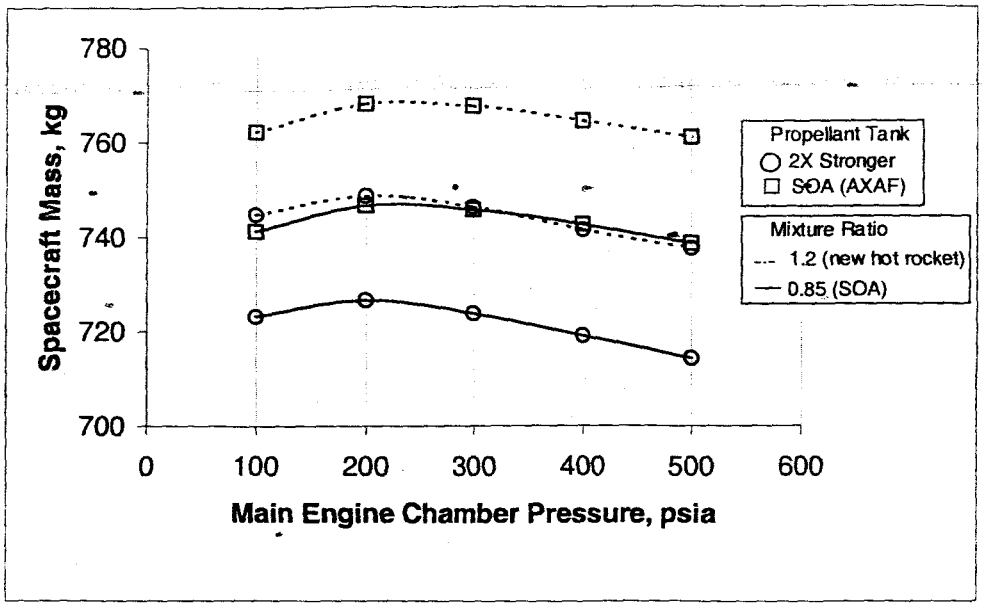

Figure 8: ACPS Payload for MR, Chamber Pressure, and Tank Technology Increases

XIV. Conclusion

The Advanced Chemical Propulsion System (ACPS) model has been created using both engineering-based models and experience-based models to allow a user to assess the impact of advanced propulsion technologies on selected missions. Parametric descriptions of a wide range of propulsion systems were used to develop certain subsystems of the model. Selected examples have shown the capability of the model to determine changes in propulsion technologies at the system level.

References

1. Mayer, N. L., Advanced X-ray Astrophysics Facility-Imaging (AXAF-I) Propulsion Subsystem, AIAA 96-2869, 32nd AIAA/ASME/SAE/ASEE Joint Propulsion Conference & Exhibit, Lake Buena Vista, FL., 1996.

2. NASA DPD692 SE09, Advanced X-ray Astrophysics Facility Mass Properties Report, March, 1999.

3. Barber, T. J. and Cowley, R. T., Initial Cassini Propulsion System In-flight Characterization, AIAA 2002-4152, 38th AIAA/ASME/SAE/ASEE Joint Propulsion Conference & Exhibit, Indianapolis, IN., 2002.

4. Leeds, M. W., Eberhardt, R. N., and Berry, R. L., Development of the Cassini Spacecraft Propulsion Subsystem, AIAA 96-2864, 32nd AIAA/ASME/SAE/ASEE Joint Propulsion Conference & Exhibit, Lake Buena Vista, FL., 1996.

5. Personal Communication, Gamber, T., Lockheed Martin Corporation, January, 2004.

6. Honda, L., Calvignac, J., and Matuszak, L., Storable Thruster Technology Program-Mission Study, The 2002 JANNAF Propulsion Meeting, 2002.

7. http://www.psi-pci.com/Data_Sheet_Index_PMD-VOL.htm, Pressure Systems Inc., March, 2004.

8. *NASA Pressurization Systems Design Guide, Volume 1 – System Analysis and Selection*, NASA-CR-80317.

9. Personal Communication, G. Woodcock, April, 2003.

10. Wu, P.-K., et al., Qualification Testing of a 2nd Generation High Performance Apogee Thruster, AIAA 2001-3253, 37th AIAA/ASME/SAE/ASEE Joint Propulsion Conference & Exhibit, Salt Lake City, UT, 2001.

11. Krismer, D., et al., Qualification Testing of a High Performance Bipropellant Rocket Engine Using MON-3 and Hydrazine, AIAA 2003-4775, 39th AIAA/ASME/SAE/ASEE Joint Propulsion Conference & Exhibit, Huntsville, AL, 2003.

12. Schneider, S. J., On-Board Propulsion System Analysis of High Density Propellants, AIAA 98-3670, 34th AIAA/SAME/SAE/ASEE Joint Propulsion Conference & Exhibit, Cleveland, OH, 1998.

13. ter Brake, H. J. M. and Wiegerinck, G. G. M., Low-power Cryocooler Survey, *Cryogenics*, 42, 705-718, 2002.

14. Glaister, D. S, Donabedian, M., Curran, D. G. T., and Davis, T., An Assessment of the State of Cryocooler Technology for Space Applications, The Aerospace Corporation, Report No. TOR-98 (1057)-3, 1998.

15. Juhasz, A. J., Tew, R. C., and Thieme, L. G., Parametric Study of Radiator Concepts for a Stirling Radioisotope Power System Applicable to Deep Space Missions, NASA/TP-2000-209676, 2000.

16. Honda, L., Calvignac, J., and Matuszak, L., Storable Thruster Technology Program-Mission Study, The 2002 JANNAF Propulsion Meeting, 2002.